Acta Crystallographica Section D
**Biological Crystallography**
ISSN 0907-4449

# Crystallographic analysis of family 11 endo-$\beta$-1,4-xylanase Xyl1 from *Streptomyces* sp. S38

**J. Wouters,[a]† J. Georis,[b]‡ D. Engher,[b] J. Vandenhaute,[a] J. Dusart,[b] J. M. Frere,[b] E. Depiereux[a] and P. Charlier[b]**

[a]Unité de Recherche en Biologie Moléculaire, Facultés Universitaires Notre Dame de la Paix, 61 Rue de Bruxelles, B-5000 Namur, Belgium, and [b]Centre d'Ingénierie des Protéines and Laboratoire d'Enzymologie, Institut de Chimie B6, Université de Liège, Sart-Tilman, B-4000 Liège, Belgium

† Present address: Institut de Recherches Microbiologiques Jean-Marie Wiame, 1 Avenue E. Gryzon, 1070 Brussels, Belgium
‡ Present address: Beldem SA, Rue Bourrie 12, B-5300 Andenne, Belgium.

Correspondence e-mail: johan.wouters@fundp.ac.be

Received 27 June 2001
Accepted 14 September 2001

**PDB Reference:** Xyl1, 1hix.

Family 11 endo-$\beta$-1,4-xylanases degrade xylan, the main constituent of plant hemicelluloses, and have many potential uses in biotechnology. The structure of Xyl1, a family 11 endo-xylanase from *Streptomyces* sp. S38, has been solved. The protein crystallized from ammonium sulfate in the trigonal space group $P321$, with unit-cell parameters $a = b = 71.49$, $c = 130.30$ Å, $\gamma = 120.0^\circ$. The structure was solved at 2.0 Å by X-ray crystallography using the molecular-replacement method and refined to a final $R$ factor of 18.5% ($R_{\rm free} = 26.9\%$). Xyl1 has the overall fold characteristic of family 11 xylanases, with two highly twisted $\beta$-sheets defining a long cleft containing the two catalytic residues Glu87 and Glu177.

## 1. Introduction

Xylan, a heteroglycan composed of linear chains of xylose residues linked by $\beta$-1,4 glycosidic bonds, with a variety of substituents (Joseleau *et al.*, 1992), is the main constituent of plant hemicelluloses and constitutes more than one third of the recyclable organic carbon source on earth. The hydrolysis of the xylan backbone is performed mainly by the action of a complex set of enzymes, of which xylanases are crucial enzymes for its depolymerization. They are produced by fungi, yeast or bacteria and liberate xylo-oligosaccharides of different lengths (Biely, 1985). One of the major objectives in biotechnological research is the engineering of microbial enzymes to efficiently improve their properties for industrial processes. Endo-xylanases (Exs) have been found to present several biotechnological applications, such as cellulose pulp biobleaching (Buchert *et al.*, 1994; Georis, Giannotta *et al.*, 2000), bread-making (Courtin *et al.*, 1999) and saccharification of lignocellulosic biomass (Lee, 1997). These applications require enzymes capable of operating under different conditions (biobleaching, for instance, requires thermostable and alkali-stable enzymes). Considerable efforts are devoted to identify new xylanases or to improve the properties of existing ones in order to meet the industrial requirements. For the design and protein engineering of endo-xylanases with different characteristics, precise knowledge of their sequence and structure is of great importance. As part of our interest in adaptations of Exs to pH and temperature (Georis, de Lemos-Esteves *et al.*, 2000), we report here the 2 Å crystal structure of the family 11 endo-$\beta$-1,4-xylanase encoded by the *xyl1* gene of *Streptomyces* sp. S38.

A large number of endo-$\beta$-1,4-xylanases (E.C. 3.2.1.8) have been described, purified, characterized and sequenced from different microorganisms (Sunna & Antranikian, 1997).

Xylanases, like all $\beta$-1,4-glycan hydrolases, utilize a general acid mechanism of catalysis promoted by two acidic amino-acid residues. Based on sequence similarities and hydrophobic cluster analysis, they have been grouped in families 10 (or F) and 11 (or G) of the glycosyl hydrolases (Gilkes *et al.*, 1991; Henrissat & Davies, 1997).

Family 10 endo-$\beta$-1,4-xylanases have a molecular weight in the range 32–39 kDa. In addition to a catalytic domain, they include a cellulose-binding domain and a linker region. The structure of the catalytic domain of several family 10 xylanases has been determined by X-ray crystallography and consists of an eightfold $\beta$-barrel (Harris *et al.*, 1996). Family 10 enzymes present a greater catalytic versatility (Biely *et al.*, 1997).

On the other hand, the catalytic domains of the family 11 endo-$\beta$-1,4-xylanases (Exs 11) have a smaller molecular mass (20–22 kDa) and usually exhibit basic pI values, although acidic pI values have been observed for some fungal enzymes. The three-dimensional structures of several of these enzymes have been solved. They include the structures of Exs 11 from *Bacillus circulans* (PDB code 1bcx; Wakarchuk *et al.*, 1994), *Trichoderma reseei* XYNI (1xyn; Törrönen & Rouvinen, 1995), *T. reseei* XYNII (1xyn; Törrönen & Rouvinen, 1995), *T. harzianum* (1xyn), *Aspergillus niger* (1ukr; Krengel & Dijkstra, 1996), *A. kawachii* (1bk1; Fushinobu *et al.*, 1998), *Thermomyces lanuginosa* (1yna; Gruber *et al.*, 1998), *Paecilomyces varioti* (1pvx; Eswaramoorthy *et al.*, 1994; Kumar *et al.*, 2000), *Bacillus agaradhaerens* (1qh6; Sabini *et al.*, 1999) and *Dictyoglomus thermophilum* XynB (1f5j; McCarthy *et al.*, 2000).

All reported structures of family 11 endo-xylanases present one single (catalytic) domain with an all-$\beta$-strand 'sandwich-like' fold containing two $\beta$-sheets forming a large cleft that can accommodate the xylan polymer (Törrönen & Rouvinen, 1997; Himmel *et al.*, 1997). The active site contains two conserved glutamate residues located on either side of the extended open cleft. According to mutagenesis and mechanism-based inhibitors, these residues have been identified as a nucleophilic and acid/base catalyst (Törrönen & Rouvinen, 1997). A precise hydrogen-bond network around the catalytic residues is capable of fine-tuning the properties of endo-$\beta$-1,4-xylanase. In this context, the structures of endo-$\beta$-1,4-xylanase I from *A. niger* (Krengel & Dijkstra, 1996), of XynC from *A. kawachii* (Fushinobu *et al.*, 1998) and a mutant (N35D) of *B. circulans* xylanase (Joshi *et al.*, 2000) demonstrated that the pH optima of family 11 xylanases are well correlated with the nature of the residue adjacent to the acid/base catalyst. In xylanases that function optimally under acidic conditions this residue is aspartic acid, whereas it is asparagine in those that function under more alkaline conditions. On structural comparison with xylanases with high pH optima stability/activity, another striking feature of acidophilic enzymes is the presence of a concentration of numerous acidic residues on the surface of the protein. At least in the case of XynC from *A. kawachii*, these acidic residues on the so-called 'Ser/Thr surface' and in the active-site cleft seem to be important for the acid stabilization of the proteins (Fushinobu *et al.*, 1998).

Other noticeable differences among family 11 endo-xylanases are the length of the N-terminal part of the protein, potentially introducing an additional $\beta$-strand in the first $\beta$-sheet, and the presence of a disulfide bridge in some structures. This latter disulfide bridge, as well as an increased density of charged residues throughout the protein, could in part explain the thermostability of *Thermomyces lanuginosus* DSM 5726 XynA (Gruber *et al.*, 1998) and of a thermophilic xylanase from *Paecilomyces varioti* (Kumar *et al.*, 2000).

In the thermostable xylanase XynB from *Dictyoglomus thermophilum*, there are three Cys residues but no disulfide bond is formed. Curiously, two of those cysteines, which are on adjacent $\beta$-strands in the active-site region, appear close enough to form a disulfide bridge, but the electron density shows clearly that they do not (McCarthy *et al.*, 2000). Compared with other family 11 endo-xylanases, XynB has a greater proportion of polar surface and has a slightly extended C-terminus that gives additional hydrogen bonding and hydrophobic packing, potentially accounting for the enhanced thermal stability of this enzyme.

In a same way, an unusual cluster of surface aromatic residues forming sticky patches has been observed in the structure of *Bacillus* D3 endo-xylanase (Harris *et al.*, 1997) and could contribute to the thermostability of this protein. Recently, some of those structural features identified as potential contributors to improve thermostability of Exs 11 have been introduced by site-directed mutagenesis in Xyl1 of *Streptomyces* sp. S38 (Georis, de Lemos-Esteves *et al.*, 2000).

**Table 1**
Data-collection parameters and refinement details.

| | |
|---|---|
| Data collection | |
| Wavelength (Å) | 0.94398 (BM30A, ESRF) |
| Space group | *P*321 |
| Unit-cell parameters | |
| $a = b$ (Å) | 71.49 |
| $c$ (Å) | 130.30 |
| $\gamma$ (°) | 120.0 |
| Resolution (Å) | 2.0 |
| No. of reflections measured | 177572 |
| No. of unique reflections | 22088 |
| Data completeness† (%) | 82.5 (84.96) |
| $R_{\rm sym}$† (%) | 8.2 (23.6) |
| $I/\sigma(I)$† | 5.66 (3.23) |
| Wilson $B$ (Å$^2$) | 14.8 |
| Refinement | |
| Resolution range (Å) | 7.0–2.0 |
| $R_{\rm cryst}$‡ (%) [$I > 4\sigma(I)$] | 18.46 (16838) |
| $R_{\rm cryst}$‡ (%) (all data) | 20.38 (22088) |
| $R_{\rm free}$‡ (%) | 26.93 (563) |
| No. of atoms (non-H) | |
| Total | 3078 |
| Protein | 2858 |
| Water | 220 |
| Deviations from ideal geometry | |
| Bond lengths (1–2 distances) (Å) | 0.006 |
| Angles (1–3 distances) (Å) | 0.024 |
| Ramachandran analysis | |
| Residues§ in most favored region (%) | 85.8 |
| Residues in additionally allowed region (%) | 13.9 |

† Values in parentheses are for the highest resolution shell. ‡ Numbers in parentheses are the number of reflections. § 302 non-Gly and non-Pro residues.

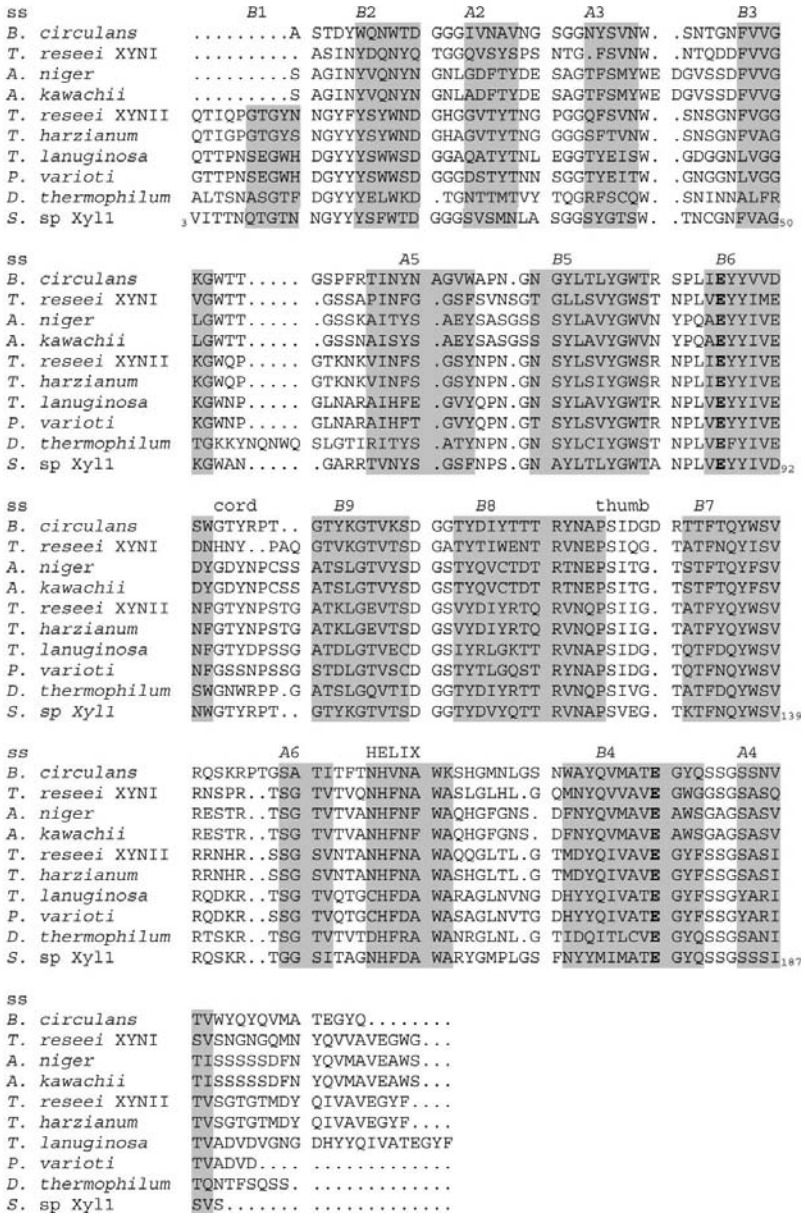


**Figure 1**
Amino-acid (one-letter code) sequence alignment of family 11 endo-xylanases. Secondary-structure elements (ss) are given at the top of the alignments. Secondary-structure elements have been numbered according to the crystal structures of *T. reseei* xylanases I and II (Törrönen & Rouvinen, 1995). Coordinates of the proteins are available in the Protein Data Bank: *B. circulans* (1bcx), *T. reseei* XYNI (1xyn), *T. reseei* XYNII (1xyp), *T. harzianum* (1xnd), *A. niger* (1ukr), *A. kawachii* (1bk1), *T. lanuginosa* (1yna), *P. varioti* (1pvx), *D. thermophilum* XynB (1f5j). The two catalytic Glu residues are marked in bold.

## 2. Materials and methods

### 2.1. Data collection and structure solution

Details about overproduction and purification of the family 11 endo-$\beta$-1,4-xylanase encoded by the *xyl1* gene of *Streptomyces* sp. S38 have been reported elsewhere (Georis *et al.*, 1999). Initial screening for crystallization conditions was performed using the vapour-diffusion technique at room temperature with several Hampton Research crystallization kits (GridScreen 6K, 6K + LiCl, NaCl, MPD, AS, PEG ion Screen, Quick Screen, Crystal Screens I and II). Clusters of small twinned hexagonal plate-shaped crystals appeared in various very different conditions. Surprisingly, it was observed that spontaneous nucleation occurred at high protein concentration, even in pure water. By either lowering the protein concentration to 1–3 mg ml$^{-1}$ or centrifugating protein samples concentrated to 10 mg ml$^{-1}$ at high speed, lower nucleation rate and larger crystals could be obtained. Reducing the precipitant agent concentration and/or the speed of vapour-diffusion equilibrium yielded the best X-ray diffraction quality crystals. The crystal used for this study was obtained in 0.8 *M* $(NH_4)_2SO_4$ buffered with 0.1 *M* sodium citrate pH 5.0 and transferred in the same mother liquor containing 30% glycerol as cryoprotectant. A complete data set (2 Å) has been collected at the ESRF (beamline BM30A) from this flash-cooled (100 K) hexagonal crystal of Xyl1, measuring about 0.4 × 0.4 × 0.05 mm, on a MAR imaging-plate area-detector system (240 mm diameter) at a wavelength of 0.94398 Å. Each diffraction data frame was exposed for 20 s for a total of 80° (1° oscillation per frame). Intensity data were integrated, scaled and reduced to structure-factor amplitudes with the *HKL* suite of programs (Otwinowski & Minor, 1997). Table 1 gives the main data-collection parameters.

The structure has been solved by molecular replacement with the program *AMoRe* (Navaza, 1994) assuming two different molecules in the asymmetric unit. First trials using the coordinates of endo-xylanase of *B. circulans* (1bcx) failed. As a search structure for molecular-replacement analysis, a model of Xyl1 was built based on the coordinates of other family 11 endo-xylanases. To build the molecular model of Xyl1, the known three-dimensional structures of Exs 11 were superimposed to delineate structurally conserved regions. The alignment of the sequences of those enzymes, presented in Fig. 1, reveals strong sequence similarities and served as the starting point for the modelling of Xyl1. Details of the homology-modelling procedure have been presented elsewhere (Georis, de Lemos-Esteves *et al.*, 2000).

The search model contained only residues 50–180 of theXyl1 sequence. The rotation function, calculated at 3.0 Å, gave two strong peaks. The translation function was then run on these solutions to search for the corresponding translation solutions (*R* factor 55.5%, correlation coefficient 19.5%). Rigid-body refinement using *AMoRe* reduced the *R* value for the two solutions to 43.6%.

Molecular packing was verified by visual inspection on the graphics screen after application of the symmetry elements

(*P*321 space group) to the coordinates of the two molecules of the asymmetric unit. Since no clashes between molecules were observed, crystal packing seemed possible in principle. This solution was used as input for the refinement.

### 2.2. Refinement

The initial model was subjected to rigid-body, simulated-annealing and positional refinement using *X-PLOR* and *CNS* (Brünger, 1992; Brunger *et al.*, 1998). At this point, $2F_o - F_c$ and $F_o - F_c$ electron-density maps were calculated. The missing residues were built step by step into the electron-density maps with the program *TURBO-FRODO* (Cambillau *et al.*, 1997). Density-modification map (*DM* program; Cowtan & Main, 1998) averaging improved the quality of electron-density maps and allowed slow reconstruction of almost the entire protein sequence. Once most of the N-terminal residues of both molecules of the asymmetric unit were located, refinement was carried out using *SHELXL* (Sheldrick & Schneider, 1997). 5% of the data were kept for the $R_{\rm free}$ test. Non-crystallographic symmetry restraints were applied. The structural models were examined periodically during refinement with $F_o - F_c$, $2F_o - F_c$, $3F_o - F_c$ and fragment-deleted difference electron-density maps. Manual adjustments were made as necessary and solvent molecules were identified. The validity of solvent molecules was assessed based on hydrogen-bonding potential to appropriate protein atoms, examination of electron-density maps and refinement of thermal factors less than 75 Å$^2$.

Disorder has been introduced for three side chains (Thr9, Ser18 and Ser40 of chain *B*) when clearly visible in difference electron-density maps (above 2.5$\sigma$), assigning half occupancy to both alternative positions. In the final model, N-terminal and C-terminal residues (Asp1, Thr2, Val3, Val189 and Ser190 for chain *A*, and Asp1, Thr2 and Ser190 for chain *B*) were omitted from the structure, as the density was too weak to define their positions with confidence. The refined structure (final *R* factor of 0.185 and $R_{\rm free}$ of 0.269) consists of 372 (185 + 187) of the 380 (2 × 190) amino-acid residues and 220 water molecules.

The overall geometry of the model is good, as judged from the r.m.s. deviation from ideal geometry of 0.006 and 0.024 Å for bond lengths (1–2 distances) and angles (1–3 distances), respectively. The average *B* value is 23.5 Å$^2$ for all protein atoms and 31.6 Å$^2$ if the 220 solvent molecules are included (Fig. 2). A Ramachandran plot was calculated for both molecules of Xyl1 in the asymmetric unit cell using the program *PROCHECK* (Laskowski *et al.*, 1993). Only Gln180 of chain *B* lies in a 'disallowed' region. Pro84 is in the *cis* conformation (in other Exs 11s, proline residues corresponding to Pro84 are also in the *cis* conformation).

Coordinates and structure-factor amplitudes have been deposited *via* the *EBI* deposition procedure in the Protein Data Bank with identification code 1hix.

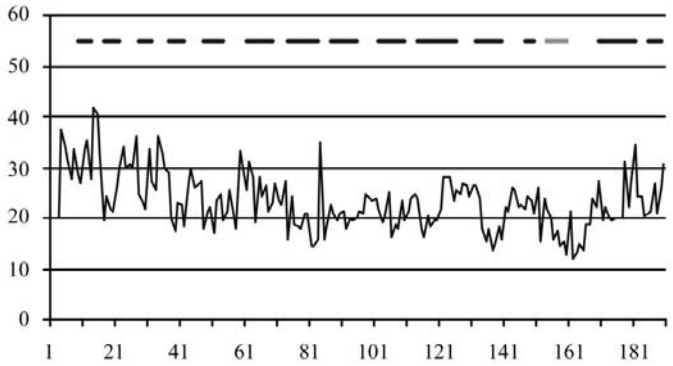


**Figure 2**
Mean *B* values for the final model of Xyl1 (only one molecule is presented, chain *A*) from *Streptomyces* sp. S38 as a function of residue number. Similar values are found for the second molecule in the asymmetric unit cell. Secondary elements are marked on the graph by lines.

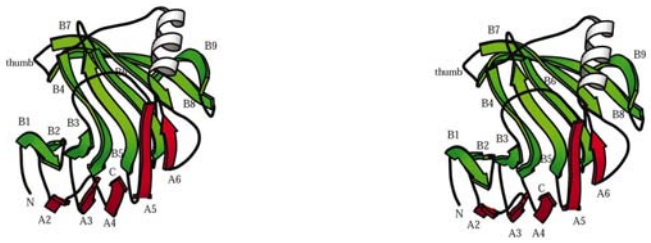


**Figure 3**
Stereoview of the overall structure of Xyl1 from *Streptomyces* sp. S38. Secondary-structure elements have been numbered according to the crystal structures of *T. reseei* xylanases I and II (Törrönen & Rouvinen, 1995). The figure was obtained with the help of the *MOLSCRIPT* program (Kraulis, 1991).

## 3. Results and discussion

### 3.1. Overall structure

The overall structure of xyl1 has a characteristic fold (Fig. 3) which is unique to family 11 endo-xylanases and has the shape of a right hand, as first described by Törrönen & Rouvinen (1995) for the structure of XYNII from *T. reesei*.

Both molecules in the asymmetric unit adopt the same conformation, the superposition of their C$^\alpha$ atoms revealing a r.m.s. deviation of the coordinates of 0.344 Å. Therefore, most of the further discussions are based on the coordinates of one (chain *A*) of the two molecules of Xyl1.

The structure of Xyl1 comprises a single domain and contains one $\alpha$-helix and 14 $\beta$-strands. The $\beta$-strands are arranged in two mostly antiparallel $\beta$-sheets. Sheet *B* is highly twisted and forms the long cleft defining the active site. The only $\alpha$-helix is embedded on the external side of this sheet.

The coiled regions are in general short and just provide short links (reverse turns and type II turns) between two $\beta$-strands. Pro84, which adopts a *cis* conformation, is involved in one of those short connections (between *B*5 and *B*6). As seen from Fig. 1, this proline residue is conserved among the Exs 11. Although most of the loop regions are rather limited in size, some longer coiled stretches are found, in particular the so-called cord region (residues 95–100). XynB of *D. thermophilium* is clearly different from the other endo-xylanase

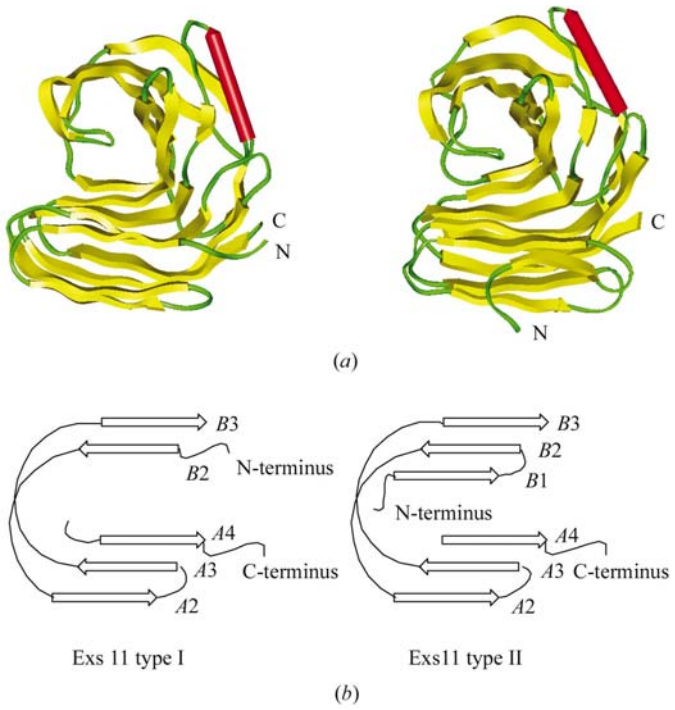


**Figure 4**
(*a*) Topologies of family 11 endo-xylanases allowing the separation of those enzymes into two groups. Exs 11 type I: endo-xylanases from *T. reseei* XYNI (1xyn), *A. niger* (1ukr), *A. kawachii* (1bk1), *B. circulans* (1bcx). Exs 11 type II: endo-xylanases from *T. reseei* XYNII (1xyp), *T. lanuginosa* (1yna), *T. harzianum* (1xnd), *P. varioti* (1pvx), *B. agaradhaerens* (1qh6), *D. thermophilum* XynB (1f5j). An enlargement of the arrangement of the secondary elements around the N-terminal region of Exs 11 is presented in (*b*).

structures in the loop connecting strand *B*3 to strand *B*5 (L5, residues 53–59). An insertion of five extra residues in this loop in XynB causes those residues to adopt a different conformation, introducing a $3_{10}$-helix and forcing the *L*5 loop as a whole to fold back against the body of the molecule, burying several hydrophobic residues.

The loop and turn regions of Xyl1 from *Streptomyces* sp. S38 are characterized by higher temperature factors, while low *B*-factor regions correlate well with secondary-structure elements (Fig. 2). During the refinement, loops *L*5 (residues 53–59) and *L*13 (residues 150–158) had to be rebuilt, as the starting conformation from the search model used in the molecular-replacement process did not fit the electron density well. After rebuilding, the two loops *L*5 and *L*13, which are spatially close to each other, appear to have a different conformation from that observed in other family 11 endo-xylanases. A similar conclusion holds for the so-called 'cord' region. As could be deduced from the sequence alignment (Fig. 1), the cord region of Xyl1, composed of six residues (residues 95–101, Gly-Thr-Tyr-Arg-Pro-Thr), most closely resembles the corresponding structure of EX11 of *B. circulans*. For other endo-xylanases, although the cord regions share a similarity in amino-acid sequence, the position of the similar residues are different. This observation had previously been made for the enzymes XYLI and XYLII of *T. reseei* (Törrönen & Rouvinen, 1995). The differences in conformations observed for the cord region can be attributed to the absence of hydrogen bonds between the cord and the rest of the molecule, this short segment of the protein being stabilized only by hydrophobic contacts.

### 3.2. N-terminal region

The topology of the secondary-structure elements of Xyl1 from *Streptomyces* sp. S38 is compared with those of related family 11 endo-xylanases in Fig. 4. The major differences between those proteins is the presence (or absence) of the *B*1 $\beta$-strand. Endo-xylanases lacking this first $\beta$-strand [*e.g.* proteins from *T. reseei* XYNI (1xyn), *A. niger* (1ukr), *A. kawachii* (1bk1) and *B. circulans* (1bcx)] position their N-terminal residues close to the C-terminal residue (Exs 11 type I; Fig. 4), in contrast to those containing this *B*1 $\beta$-strand [*e.g.* proteins from *T. reseei* XYNII (1xyp), *T. harzianum* (1xnd), *T. lanuginosa* (1yna), *P. varioti* (1pvx), *B. agaradhaerens* (1qh6) and *D. thermophilum* XynB (1f5j)] (Exs 11 type II; Fig. 4). The structure of Xyl1 belongs to the type II family 11 endo-xylanases, as it contains *B*1. These differences contribute to structural stabilization of the family 11 xylanases. Indeed, several independant studies showed that mutations in the N-terminal sequence of Exs 11 increase the thermostability and thermophilicity of those proteins (Sung *et al.*, 1998; Shibuya *et al.*, 2000; Georis, de Lemos-Esteves *et al.*, 2000).

Intramolecular hydrogen bonds stabilize the N-terminal region of Xyl1. The pattern of hydrogen bonds involving the main-chain NH and C=O groups in that region is characteristic of those observed in antiparallel $\beta$-sheets. Interestingly, residue Gly4 is also stabilized by hydrogen bonding to Met29 (belonging to the *A* sheet). Residues 3, 4 and 5 adopt a coplanar all-*trans* conformation of the main chain. No coordinates for the two first N-terminal residues could be assigned unambigously in the electron-density maps. Hydrogen bonds involving side chains play an additional role in the stabilization of the loop conformations. Conformation

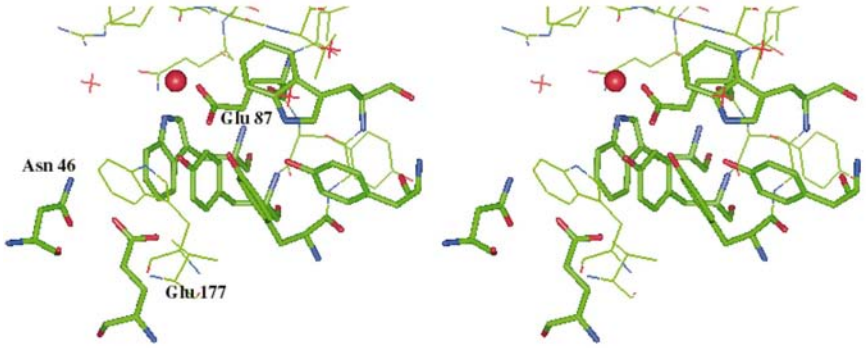


**Figure 5**
Stereoview of the active site of Xyl1 from *Streptomyces* sp. S38.

of the loop region composed of residues Thr5, Thr6 and Asn7 is imposed by hydrogen bonds involving the side chains of Thr6 and Gln8.

In a similar way, the loop region between *B*1 and *B*2, composed of residues Asn13, Gly14 and Tyr15, is stabilized by hydrogen bonds involving the main-chain carbonyl C=O of Asn12 and NH main-chain functions of Asn13 and Gly14 plus interaction of the lateral chain of Asn13 (stabilized by a hydrogen bond to residue 32).

### 3.3. Environment of catalytic glutamic acid residues

By analogy with the other family 11 endo-xylanases, the two catalytic acid groups in Xyl1 are provided by two catalytic glutamic acid residues (Glu87 and Glu177; Fig. 5) situated at the bottom of the cleft. They are separated by 5.9 and 6.5 Å, for chain *A* and *B*, respectively, consistent with other structures of endo-xylanases. Indeed, the distance between the catalytic acid groups is of the same length in the potential active conformation observed in the xylanases from *B. circulans* (5.9 Å), *T. reesei* I (6.7 Å) and *T. harzianum* (6.4 Å). In the *T. lanuginosus* and *T. reesei* II enzymes, where this distance is longer (10.7 and 10.9 Å, respectively), a conformational change is expected to generate a catalytically active species. We conclude therefore that Glu87 and Glu177 in Xyl1 from *Streptomyces* sp. S38 are in the active conformation.

The catalytic Glu residues are further connected *via* hydrogen bonding to a water molecule. In general, the structure and interactions in the Xyl1 active site match the other family 11 xylanases very closely. Those interactions involve residues that are fully conserved in the other endo-xylanases, with one exception, residue Asn46, which is substituted by an aspartic acid residue in enzymes with a low pH optimum (Krengel & Dijkstra, 1996). In Xyl1, this Asn46 points into the active site and is connected to Glu177 (3.6 and 3.8 Å, for chains *A* and *B*, respectively).

It has been proposed that the guanidinium group of Arg121 is close enough to Glu87 to maintain a low p$K_a$ for this acid group. In Xyl1, the distance between the side chain of Arg121 and Glu87 (measured between CZ 121 and CD 87) is 7.3 Å in molecule *A* and 7.1 Å in molecule *B*. This distance varies in different family 11 endo-xylanases, underlying the flexibility of this conserved residue Arg121. Therefore, it is postulated that the binding of a substrate may induce a repositioning of the Arg121 guanidinium group and thus modulate its involvement in the catalytic mechanism.

A series of conserved aromatic residues line at the base of the cleft. The position and orientation of those conserved active-site residues in Xyl1 and in other EX11s are quite similar. They define the substrate/inhibitor-binding site, confirming the hypothesis made by others that the substrate-binding site of family 11 endo-xylanases is essentially preformed (Sabini *et al.*, 1999; McCarthy *et al.*, 2000).

The authors thank Dr Josette Lamotte-Brasseur for providing coordinates of the search model used in molecular replacement. Part of the project received financial support from the Région Wallonne as a 'Bioval project' conventions No. 981/3860, 991/4023 and 991/4024. The authors also acknowledge the local contacts on the French CRG beamline BM30-ESRF (Grenoble) for advice during data collection and processing.

## References

Biely, P. (1985). *Trends Biotechnol.* **3**, 286–290.
Biely, P., Vrsanská, M., Tenkanen, M. & Kluepfel, D. (1997). *J. Biotechnol.* **57**, 151–166.
Brünger, A. T. (1992). *Nature (London)*, **355**, 472–474.
Brunger, A. T., Adams, P. D., Clore, G. M., Delano, W. L., Gros, P., Grosse-Kunstleve, R. W., Jiang, J.-S., Kuszewski, J., Nilges, M., Pannu, N. S., Read, R. J., Rice, L. M., Simonson, T. & Warren, G. L. (1998). *Acta Cryst.* D**54**, 905–921.
Buchert, J., Tenkanen, M., Kantelinen, A. & Viikari, L. (1994). *Bioresource Technol.* **50**, 65–72.
Cambillau, C., Roussel, A., Inisan, A. G. & Knoops-Mouthuy, E. (1997). *TURBO-FRODO*. University of Aix-Marseille, France.
Courtin, C. M., Roelants, A. & Delcour, J. A. (1999). *J. Agric. Food Chem.* **47**, 1870–1877.
Cowtan, K. & Main, P. (1998). *Acta Cryst.* D**54**, 487–493.
Eswaramoorthy, S., Vithayathil, P. J. & Viswamitra, M. A. (1994). *J. Mol. Biol.* **243**, 806–808.
Fushinobu, S., Ito, K., Konno, M., Wakagi, T. & Matsuzawa, H. (1998). *Protein. Eng.* **11**, 1121–1128.
Georis, J., Giannotta, F., De Buyl, E., Granier, B. & Frere, J. M. (2000). *Enzyme Microb. Technol.* **26**, 178–186.
Georis, J., Giannotta, F., Lamotte-Brasseur, J., Devreese, B., van Beeumen, J., Granier, B. & Frere, J. M. (1999). *Gene*, **237**, 123–133.
Georis, J., de Lemos-Esteves, F., Lamotte-Brasseur, J., Bougnet, V., Devreese, B., Giannotta, F., Granier, B. & Frere, J. M. (2000). *Protein Sci.* **9**, 466–475.
Gilkes, N. R., Henrissat, B., Kilburn, D. G., Miller, R. C. Jr & Warren, R. A. J. (1991). *Microbiol. Rev.* **55**, 303–315.
Gruber, K., Klintschar, G., Hayn, M., Schlacher, A., Steiner, W. & Kratky, C. (1998). *Biochemistry*, **37**, 13475–13485.
Harris, G. W., Jenkins, J. A., Connerton, I. & Pickersgill, R. W. (1996). *Acta Cryst.* D**52**, 393–401.
Harris, G. W., Pickersgill, R. W., Connerton, I., Debeire, P., Touzel, J.-P., Breton, C. & Pérez, S. (1997). *Proteins*, **29**, 77–86.
Henrissat, B. & Davies, G. (1997). *Curr. Opin. Struct. Biol.* **7**, 637–644.
Himmel, M. E., Karplus, P. A., Sakon, J., Adney, W. S., Baker, J. O. & Thomas, S. R. (1997). *Appl. Biochem. Biotechnol.* **63**, 315–325.
Joseleau, J. P., Comptat, J. & Ruel, K. (1992). *Xylans and Xylanases*, edited by J. Visser, G. Beldman, M. A. Kusters-Van Someren & A. G. J. Voragen, pp. 1–15. Amsterdam: Elsevier.
Joshi, M. D., Sidhu, G., Pot, I., Brayer, G. D., Withers, S. G. & McIntosh, L. P. (2000). *J. Mol. Biol.* **299**, 255–279.
Kraulis, P. J. (1991). *J. Appl. Cryst.* **24**, 946–950.
Krengel, U. & Dijkstra, B. (1996). *J. Mol. Biol.* **263**, 70–78.
Kumar, P. R., Eswaramoorthy, S., Vuthayathil, P. J. & Viswamitra, M. A. (2000). *J. Mol. Biol.* **295**, 581–593.
Laskowski, R. A., MacArthur, M. W., Moss, D. S. & Thornton, J. M. (1993). *J. Appl. Cryst.* **26**, 283–291.
Lee, J. (1997). *J. Biotechnol.* **56**, 1–24.
McCarthy, A., Morris, D., Bergquist, P. & Baker, E. (2000). *Acta Cryst.* D**56**, 1367–1375.
Navaza, J. (1994). *Acta Cryst.* A**50**, 157–163.
Otwinowski, Z. & Minor, W. (1997). *Methods Enzymol.* **276**, 307–326.
Sabini, E., Sulzenbacher, G., Dauter, M., Dauter, Z., Jorgensen, P. L., Schülein, M., Dupont, C., Davies, G. J. & Wilson, K. S. (1999). *Chem. Biol.* **6**, 483–492.
Sheldrick, G. M. & Schneider, T. R. (1997). *Methods Enzymol.* **277**, 319–343.

Shibuya, H., Kaneko, S. & Hayashi, K. (2000). *Biochem J.* **349**, 651–656.
Sung, W. L., Yaguchi, M. & Ishikawa, K. (1998). US Patent 5759840.
Sunna, A. & Antranikian, G. (1997). *Crit. Rev. Biotechnol.* **17**, 39–67.
Törrönen, A. & Rouvinen, J. (1995). *Biochemistry*, **34**, 847–856.
Törrönen, A. & Rouvinen, J. (1997). *J. Biotechnol.* **57**, 137–149.
Wakarchuk, W. W., Campbell, R. L., Sung, W. L., Davoodi, J. & Yaguchi, M. (1994). *Protein Sci.* **3**, 467–475.